Applied Surface Science 391 (2017) 33–38

Contents lists available at ScienceDirect

Applied Surface Science

journal homepage: www.elsevier.com/locate/apsusc

# Phase-field simulations of faceted Ge/Si-crystal arrays, merging into a suspended film

Marco Salvalaglio[a,*], Roberto Bergamaschini[a], Rainer Backofen[b], Axel Voigt[b], Francesco Montalenti[a], Leo Miglio[a]

[a] L-NESS and Department of Materials Science, Università di Milano-Bicocca, Via R. Cozzi 55, I-20126 Milano, Italy
[b] Institut für Wissenschaftliches Rechnen, Technische Universität Dresden, D-01062 Dresden, Germany

ARTICLE INFO

*Article history:*
Received 14 December 2015
Received in revised form 11 May 2016
Accepted 14 May 2016
Available online 18 May 2016

*Keywords:*
Heteroepitaxy
Surface diffusion
Phase field
Germanium
Surface energy

ABSTRACT

We simulate the morphological evolution of Ge microcrystals, grown out-of-equilibrium on deeply patterned Si substrates, as resulting from surface diffusion driven by the tendency toward the minimization of the surface energy. In particular, we report three-dimensional phase-field simulations accounting for the realistic surface energy anisotropy of Ge/Si crystals. In Salvalaglio et al. (2015) [10] it has been shown both by experiments and simulations that annealing of closely spaced crystals leads to a coalescence process with the formation of a suspended film. However, this was explained only by considering an isotropic surface energy. Here, we extend such a study by showing first the morphological changes of faceted isolated crystals. Then, the evolution of dense arrays is considered, describing their coalescence along with the evolution of facets. Combined with the previous results without anisotropy in the surface energy, this work allows us to confirm and assess the key features of the coalescence process.

## 1. Introduction

Heteroepitaxy of semiconductors is widely exploited to improve the performances of opto- and micro-electronic devices. A well-known example is represented by $Si_{1-x}Ge_x$ films grown on Si(001) substrates, as they are a key for the heterogeneous integration of electronic components in the Si-based technology [1]. Indeed, the Ge/Si system, characterized by both lattice (4.2%) and thermal (130%) misfit, can be considered a prototype for the investigation of more complex configurations involving other materials. In close-to-equilibrium conditions, i.e. high temperatures and low deposition fluxes, the growth of Ge films on Si is initially characterized by the formation of self-assembled three-dimensional (3D) islands, following the so-called Stranski–Krastanov growth modality [2,3]. At later stages, the insertion of linear defects, i.e. dislocations, is eventually observed [4]. For deposition rates (and/or temperatures) high (low) enough to substantially reduce the surface diffusion length, i.e. in out-of-equilibrium conditions, the formation of planar films is achieved from the very beginning, relaxing the lattice strain by the insertion of misfit dislocations [5]. Still, two main technological problems are encountered. First, the misfit segments of dislocations at the Ge/Si interface terminate at the film surface by threading arms, which are very detrimental for the performances of devices. Second, thick-enough films generate wafer warping and cracks, due to the different thermal expansion coefficients of Si and Ge [6].

Recently, vertical 3D Ge (or $Si_{1-x}Ge_x$) crystals on deeply patterned Si substrates have been demonstrated at the micron scale by Low Energy Plasma Enhanced Chemical Vapor Deposition (LEPECVD) [7]. In contrast with the growth on planar substrates, separated crystals were obtained with large height-to-base aspect ratios and peculiar 3D morphologies characterized by a complex faceting [8]. This was achieved thanks to the out-of-equilibrium conditions ensured by LEPECVD. In particular, the growth kinetics was mainly determined by both the orientation-dependent incorporation rate and the mutual shielding of the incoming material flux [7,8]. Such vertical structures were proved to be of very high crystalline quality [7]. Moreover, thanks to their high aspect-ratio, they permit to confine dislocations threading arms in the lower part of the crystals [9] and fully relax thermal strain [7].

In Ref. [10] we investigated the evolution of these vertical Ge/Si heterostructures induced by annealing. The coalescence of closely spaced crystals was reported, providing a viable path for the formation of high-quality suspended networks, with promising properties for the heterogeneous integration of semiconductors. This mechanism was explained by taking into account the thermally-activated surface diffusion [11,12], driven by the

---

* Corresponding author. Present address: Institut für Wissenschaftliches Rechnen, Technische Universität Dresden, D-01062 Dresden, Germany.
*E-mail address:* marco.salvalaglio@tu-dresden.de (M. Salvalaglio).

http://dx.doi.org/10.1016/j.apsusc.2016.05.075

tendency toward the minimization of the surface energy only. Indeed, at variance with standard heteroepitaxy [13], the elastic energy contribution is typically negligible in Ge/Si vertical crystals thanks to the peculiar elastic and plastic relaxation mechanisms [7,14]. Moreover, Si and Ge form almost ideal alloys with no enthalpy of mixing and the alloying due to entropic contribution can occur only by bulk diffusion during annealing. Therefore, it is limited to a small region of a few monolayers at the Ge/Si interface [13], not influencing the evolution of the Ge surface. Dedicated simulations were performed exploiting a 3D Phase-Field (PF) model [15]. Such an approach was selected to conveniently tackle the evolution of complex geometries, also in the presence of major topological changes. For the sake of simplicity, however, only isotropic surface energy was there considered.

Thus, the evolution of Ge microstructures was qualitatively described by neglecting any dependence of the surface energy on the local orientation $\hat{\mathbf{n}}$ [10], although crystals are known to exhibit preferential faceting which results from anisotropic surface energy densities $\gamma(\hat{\mathbf{n}})$ [16,17]. In general, once $\gamma(\hat{\mathbf{n}})$ values are known, the Equilibrium Crystal Shape (ECS) can be obtained by means of the so-called Wulff construction [18,19]. However, more advanced tools are required to describe the changes in the faceting of crystals during the evolution towards the equilibrium [20]. Despite the initial faceting of Ge microcrystals is determined by the growth kinetics [8], the surface-energy dependence on $\hat{\mathbf{n}}$ is expected to become important for high-temperature treatments, as close-to-equilibrium conditions are achieved. Indeed, experiments clearly show changes in the faceting during post-growth annealing processing. Actually, new facets characteristic of the ECS appear, which are absent in the as grown profile [10].

The PF framework deals with the description of surface diffusion evolution in the presence of an anisotropic $\gamma(\hat{\mathbf{n}})$ [15]. This holds true also in the strong anisotropy regime, i.e. when sharp corners appear in the ECS and a proper energy regularization should be adopted as the evolution equations become ill-defined [21]. Moreover, such an approach has been demonstrated to tackle the 3D evolution of realistic faceted morphologies [22]. As far as we are just focusing on the case of annealing, the growth dynamics of the vertical crystals is neglected. However, this could be straightforwardly included in the PF approach by adding an external flux term, eventually accounting for kinetic anisotropy as, for instance, in Refs. [23,24]. The role of these two competing terms in driving the crystals coalescence was discussed in Ref. [25] also in comparison with experiments, and the modeling of the growth dynamics reported therein could represent a natural extension of the PF approach.

At variance from Ref. [10], in this work we aim to provide a more realistic description of the crystal coalescence by explicitly accounting for the anisotropy in the surface energy, responsible for the faceting in the thermodynamic regime of annealing. This provides a better match to the experimental evidence and permits a deeper understanding of the mechanisms behind coalescence. In particular, we first discuss the definition of a continuous $\gamma(\hat{\mathbf{n}})$ function, obtained by interpolating the values of the known preferential orientations of Ge crystals reported in literature [16]. PF simulations of surface diffusion accounting for this definition of $\gamma(\hat{\mathbf{n}})$ are then performed to assess the morphological evolution of isolated microcrystals during annealing. Closely spaced crystals are finally considered in order to describe their coalescence along with the facets evolution, and the role of the surface anisotropy is discussed.

## 2. Phase-field model

In order to describe the morphological evolution by surface diffusion for 3D crystals, we adopted a continuum description based on the so-called phase-field (PF) model [15]. An auxiliary function $\varphi(\mathbf{x})$ is used as an order parameter describing the solid phase, $\varphi = 1$, and the vacuum phase, $\varphi = 0$, with a continuum variation in between. A suitable choice for $\varphi$ is given by

$$\varphi(\mathbf{x}) = \frac{1}{2}\left[1 - \tanh\left(\frac{3d(\mathbf{x})}{\epsilon}\right)\right], \tag{1}$$

with $\epsilon$ the interface thickness and $d(\mathbf{x})$ the signed distance from the surface of the solid phase, namely the $\varphi \sim 0.5$ isosurface. The evolution based on thermodynamic driving forces requires to define the free energy $F$ as a function of $\varphi$. Since the crystals are fully-relaxed from the mechanical point of view (by both plastic and elastic relaxation mechanisms), and intermixing effects can be neglected [7], only surface energy should be considered. According to Ref. [21], the energy functional is

$$F[\varphi] = \int_V \gamma(\hat{\mathbf{n}})\left(\frac{\epsilon}{2}|\nabla\varphi|^2 + \frac{1}{\epsilon}B(\varphi)\right)d\mathbf{x} + \int_V \frac{\beta}{2\epsilon}\kappa(\varphi)^2 d\mathbf{x}. \tag{2}$$

The first integral is the Ginzburg–Landau functional, with $B(\varphi) = 18\varphi^2(1-\varphi)^2$, $\gamma(\hat{\mathbf{n}})$ the surface energy density and $\hat{\mathbf{n}} = -\nabla\varphi/|\nabla\varphi|$ the outer-pointing surface normal. The second integral is the regularization required for strongly anisotropic systems, namely the Willmore regularization [21], which corresponds to an edge/corner energy term [26]. $\kappa(\varphi) = -\epsilon\nabla^2\varphi + (1/\epsilon)B'(\varphi)$ is the approximation of the curvature in the PF approach. This regularization produces a rounding of the corners controlled by the $\beta$ parameter. The surface diffusion mechanism [11,12] is then derived as an evolution law for $\varphi$ [15] as

$$\frac{\partial\varphi}{\partial t} = \nabla\cdot(M(\varphi)\nabla\mu), \tag{3}$$

with $M(\varphi) = 2M_0B(\varphi)/\epsilon$ the mobility function restricted to the surface, with $M_0$ as a scaling factor, and $\mu$ the chemical potential. The latter is defined by [21]

$$\begin{aligned} g(\varphi)\mu = \delta F/\delta\varphi = -\epsilon\nabla\cdot\left[\gamma(\hat{\mathbf{n}})\nabla\varphi\right] + \frac{1}{\epsilon}\gamma(\hat{\mathbf{n}})B'(\varphi) - \epsilon\nabla \\ \cdot\left[|\nabla\varphi|^2\nabla_{\nabla\varphi}\gamma(\hat{\mathbf{n}})\right] + \beta\left(-\nabla^2\kappa + \frac{1}{\epsilon^2}B''(\varphi)\kappa\right) \end{aligned} \tag{4}$$

with $\nabla_{\nabla\varphi}$ the gradient along the direction of $\nabla\varphi$ and $g(\varphi) = 30\varphi^2(1-\varphi)^2$ a stabilizing function included to improve the convergence of the present PF model to the surface diffusion in the sharp-interface limit ($\epsilon \to 0$) [27,28]. In the following we will consider time expressed in arbitrary units. For consistency with the Ge/Si vertical heterostructures reported in the literature, e.g. in Refs. [7,8,10], the unit of length is expressed in $\mu$m.

The numerical integration of the evolution law for $\varphi$ is obtained by solving the system of the partial differential equations for $\partial\varphi/\partial t$, $g(\varphi)\mu$ and $\kappa$. A semi-implicit integration scheme similar to the one reported in Ref. [22] is considered, with numerical stability improved by following the approach proposed in Ref. [29]. The implementation of such a framework has been performed within the AMDiS Finite Element Method toolbox [30,31], and solved by both direct and iterative solvers. In order to optimize the required calculations, a non-uniform space discretization has been adopted with refined mesh at the interface, where surface diffusion evolution is active.

## 3. Anisotropic surface energy

When considering the anisotropy of the surface energy, the data available in the literature typically consist of a discrete set of $\gamma$ values for the preferential orientations. From these data, one can calculate the expected ECS in agreement with the Wulff construction [18]. In Fig. 1a, such a shape is calculated using the Wulffmaker software [32], accounting for the main families of facets for Ge,

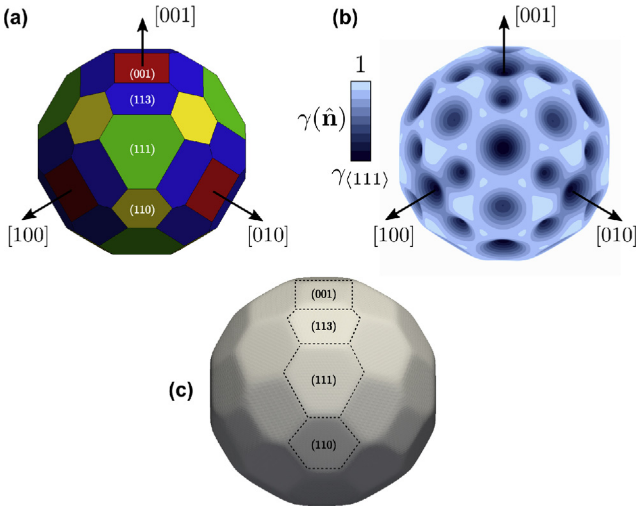

**Fig. 1.** Surface energy density and equilibrium shape. (a) Equilibrium crystal shape bounded only by {100}, {113}, {111} and {110} facets. Their extensions is set according to the surface energy density values in Ref. [16] (computed by Wulffmaker [32]) (b) $\hat{\mathbf{n}}\gamma(\hat{\mathbf{n}})$ plot of the continuous surface energy function obtained by tuning Eq. (5) with the minima of the surface energy as in panel (a). The color map shows the values of $\gamma(\hat{\mathbf{n}})$. (c) Equilibrium configuration obtained by a PF simulation of surface diffusion, in the presence of the anisotropic $\gamma(\hat{\mathbf{n}})$. Dashed lines illustrate the outline of the resulting facets.

i.e. {100}, {113}, {111} and {110}, and the corresponding surface energy values reported in Ref. [16].

The PF approach described in Section 2, however, requires a continuous $\gamma(\hat{\mathbf{n}})$ function with values for each orientation. The description of the anisotropic surface energy that we adopt here is based on the general expression of $\gamma(\hat{\mathbf{n}})$ introduced in Ref. [22], i.e.

$$\gamma(\hat{\mathbf{n}}) = \gamma_0 \left( 1 - \sum_{i=1}^{N} \alpha_i (\hat{\mathbf{n}} \cdot \hat{\mathbf{m}}_i)^{w_i} \Theta(\hat{\mathbf{n}} \cdot \hat{\mathbf{m}}_i) \right), \tag{5}$$

where $N$ is the total number of the energy minima in $\gamma(\hat{\mathbf{n}})$ along the directions $\hat{\mathbf{m}}_i$ with depth $\alpha_i$. The $w_i$ parameter controls the width of the $i$-th minimum, i.e. the range of the orientations $\hat{\mathbf{n}}$ around $\hat{\mathbf{m}}_i$ where $\gamma(\hat{\mathbf{n}})$ is lower than $\gamma_0$. For a large enough $w_i$ value, $\gamma(\hat{\mathbf{m}}_i) = \gamma_0(1-\alpha_i)$. $\Theta$ is the Heaviside step function.

The surface energy of real Ge crystals is reproduced by selecting $\hat{\mathbf{m}}_i$ and $\alpha_i$ in order to match the orientations of the minima and the surface energy values reported in the literature [16]. In particular, we focus our attention on the main preferential orientations, corresponding to {100}, {113}, {111} and {110} facets as in Fig. 1a. The energy of the facets with normal along ⟨100⟩ directions is considered as a reference, assuming $\alpha_{\langle 100\rangle} = 0.15$. The $\alpha_i$ coefficients are then obtained by

$$\alpha_i = 1 - \left( \frac{\gamma_i}{\gamma_{\langle 100\rangle}} \right) (1 - \alpha_{\langle 100\rangle}), \tag{6}$$

where $i$ indicates one of the aforementioned families of facets and $\gamma_i$ is the corresponding surface energy value reported in Ref. [16]. Notice that $\gamma_0$ is not present in Eq. (6) as it does not affect the ratio between different minima. Therefore it can be used as a scaling factor in order to match the desired magnitude of the surface energy. For the sake of simplicity we set $\gamma_0 = 1$. The $w_i$ parameter has been selected equal to 100 for minima along ⟨113⟩ directions and to 50 for the other minima to ensure no superposition of the different contributions in the sum of Eq. (5) for each $\hat{\mathbf{m}}_i$ [22].

The $\gamma(\hat{\mathbf{n}})$ resulting from such a procedure, with $\alpha_i$ values from Eq. (6), is shown in Fig. 1b. This construction of the surface energy density accounts for every possible orientation of the crystal and not only for the ones corresponding to surface energy minima. In principle, this allows for a fine tuning of $\gamma(\hat{\mathbf{n}})$ including also the energetics of the connections between facets. However, these orientations are affected by local features of the crystals such as vicinal surfaces and step bunching, which are generally unknown and difficult to be addressed. With this respect, the formulation for the $\gamma(\hat{\mathbf{n}})$ function of Eq. (5) (as shown in Fig. 1b) represents a convenient fit of a continuous function passing through the known energy minima.

The equilibrium configuration given by the $\gamma(\hat{\mathbf{n}})$ function as in Fig. 1b is shown in Fig. 1c. It is obtained by the PF model of surface diffusion described in Section 2, starting from a sphere. The initial profile is set by considering Eq. (1) with $\epsilon = 0.05$ and a signed distance defined by $d(\mathbf{x}) = |\mathbf{x}| - R$ with $R$ the radius of the sphere, set to 1 in the present simulation. Hereafter the reported surface profiles correspond to the $\varphi(\mathbf{x}) \sim 0.5$ isosurface. The regularization parameter $\beta$ is arbitrarily set to 0.003 to ensure a small rounding at corners and edges. The differences in $\gamma(\hat{\mathbf{n}})$ on the surface of the sphere induce a material flux following the gradient of the chemical potential, as described by Eq. (3), and eventually lead to the equilibrium configuration. The final shape shows a faceting of the surface resembling the morphology in Fig. 1a but it also includes the intermediate orientations with respect to the preferential ones. The regularization term in Eq. (2) avoids the presence of sharp edges and corners producing rounded connections between facets [21,22]. This leads to a slightly different shape than the one in Fig. 1a and the outlines of the facets are not sharply defined. However, the equilibrium configuration keeps all the main features obtained by the Wulff construction, as also shown by the dashed lines in Fig. 1c.

It is worth mentioning here that the evolution described by the PF model provides a real kinetic pathway towards the equilibrium crystal shape starting from any initial configuration. Moreover, the description of a realistic surface energy is included. However, the present model does not account for the possible energy barriers for the diffusion among different facets (thus assuming full activation of the diffusion processes) whose description requires a dedicated development of the PF framework considered here, out of the purposes of the present work. The assumptions of the model proved to be effective in describing the main features of the evolution by an a-posteriori comparison with the evidences in Ref. [10].

## 4. Results and discussion

As assessed in Ref. [10], the evolution in time of the 3D Ge microstructures with isotropic surface energy is mainly characterized by a rounding of the crystals, leading to the lowering of the aspect-ratios. This is the key enabling feature for the coalescence process occurring in closely-spaced crystals. When accounting for the anisotropic surface energy, as shown in Fig. 1c, facets are obtained and this may significantly affect the global rounding and the lateral expansion. Actually, some investigations have been reported in the literature describing the evolution by surface diffusion of elongated structures, such as simple rectangles or parallelepipeds, in the presence of surface faceting. Results have been obtained, for instance, by a fully-faceted approach in 2D [20] or within the PF model dealing with the 3D evolution [22]. According to these works, an enlargement of the elongated structures is still obtained also in the presence of faceting. This suggests that this feature will be also present when explicitly considering the anisotropy of $\gamma(\hat{\mathbf{n}})$ in our system of interest.

In order to investigate this behavior in the specific case of 3D Ge microcrystals, we focus on the typical experimental structures introduced in Ref. [7]. They are obtained by deposition of Ge, up to a thickness of 8 µm, on 2 µm × 2 µm wide, 8 µm tall Si pillars. In particular, we consider a realistic initial profile closely resembling the morphology of the experimental shape obtained at a growth

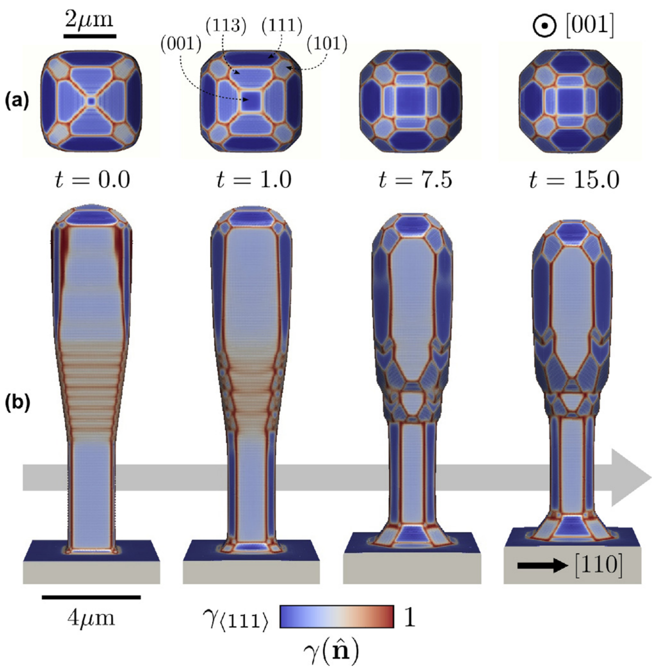

**Fig. 2.** Evolution by surface diffusion of an isolated crystal. The initial geometry is set to closely resemble the experimental one obtained at a growth temperature of ~500 °C in Refs. [7,8]. (a) Top and (b) lateral view of four representative stages are reported. The color map shows the $\gamma(\hat{\mathbf{n}})$ values. Dashed arrows mark the families of facets. Time is expressed in arbitrary units.

temperature of ~500 °C [7,8] (see $t=0$ in Fig. 2). The Si pillar below the Ge crystal is modeled as a simple cylinder where the mobility vanishes, i.e. $M_0 \sim 0$ [10]. This is justified by the very low mobility of Si compared to the Ge one [33] at the typical processing temperatures, up to ~800 °C during annealing. The presence of a small amount of Ge on the sidewalls of the Si pillar is also considered, in agreement with the experimental evidence.

The evolution by surface diffusion of such a structure with the $\gamma(\hat{\mathbf{n}})$ function defined in Section 3 is shown in Fig. 2 ($\epsilon = 0.2$). The color map shows the local $\gamma(\hat{\mathbf{n}})$ values, highlighting the presence of the facets where a uniform color is obtained at almost constant $\hat{\mathbf{n}}$. Moreover, rounded connections between facets, with high values of $\gamma(\hat{\mathbf{n}})$, are obtained as imposed by the regularization in Eq. (2) [21]. In the first stages, the original faceting resulting from the kinetic growth is modified by surface diffusion. Indeed, the pyramid bounded by {113} facets at the top of the crystal in the initial configuration, evolves into a truncated pyramid with the clear appearance of the (001) facet, as expected from the equilibrium crystal shape (see Fig. 1). This feature has been directly observed in the experiments in Ref. [10] and cannot be reproduced by the evolution with isotropic surface energy. Moreover, the facets which are stable according to the surface energy, and already present in the initial configuration, are preserved. Faceted sidewalls appear as imposed by the choice of $\gamma(\hat{\mathbf{n}})$ with also the formation of $(\pm 100)$ and $(0 \pm 10)$ facets at the vertical edges. At the bottom of the Ge crystals, where the initial profile shows unstable orientations, a complex faceting is formed involving several different facets, providing the average slope required to match the size of the Si pillar with the Ge crystal on top. A transfer of the material around the Si pedestal towards the planar substrate is also observed, until exposing the Si. Indeed, faceting at the bottom of the whole structure is observed and the height of the planar region around the structure increases. As can be noticed from Fig. 2, by comparing the first stages with the morphology at $t=15$, the global evolution leads to a lowering of the crystal which results also slightly enlarged. In agreement with the evidence reported in Ref. [10], when considering closely spaced structures separated by a few tens of nanometers, this behavior would produce the filling of the gap between the crystals. Then, coalescence occurs and the dynamics varies significantly with respect to the isolated crystals discussed so far.

The more complex evolution of crystal arrays is here investigated by focusing on the same initial geometry used for the simulations of Fig. 2, in order to reproduce an evolution as close as possible to the real systems. In particular, the initial profile consists of crystals aligned along the [110] and the $[\bar{1}10]$ directions with a periodicity equal to 4 μm. The resulting gap between the crystals is ~0.4 μm. Periodic boundary conditions are considered for the lateral boundaries of the simulation cell. The evolution for such a system is illustrated in Fig. 3, where representative stages of the PF simulations are shown. The color map shows the local $\gamma(\hat{\mathbf{n}})$ values as in Fig. 2. In the first stages of the evolution, crystals are not affected by the neighbours and the morphological changes are the same as discussed for isolated crystals ($t=1.0$, as in Fig. 2). Then, coalescence of crystals along [110] and $[\bar{1}10]$ directions is obtained with the formation of bridges in between ($t=2.5$). These regions act as sinks collecting material from the surroundings as can be appreciated by comparing the extension of the merging at $t=2.5$ and $t=6.0$. A global lowering of the upper portion of the crystal is then obtained with the disappearance of large {111} facets at the top, favoring the extension of {113} facets. Also {110} facets, which may extend due to the free surface between bridges ($t=6.0$), grow larger up to the closure of the holes while (001) facets are formed on top of the coalesced regions. At later stages the complete closure of the holes is achieved, resulting in a continuous surface with a faceted profile as shown at $t=9.5$. During this stage, new (001) facets are formed when holes are filled while the other flat regions extend. Moreover, the extension of {113} and {110} facets is gradually reduced. Eventually, the suspended film flattens and a single (001) surface is obtained on top of the structure as the final stage ($t=15$), shown in Fig. 3(a) by the last top view.

Further insights on the coalescence process can be extracted by looking at the values of the free energy in time, namely $F(t)$, with $F$ defined by Eq. (2). In Fig. 4 we show the $F(t)$ values, normalized with respect to the surface energy of the initial configuration (at $t=0$). Two abrupt changes of the slope can be easily recognized and correspond to the topological changes of the structure, i.e. the coalescence of the crystals and the filling of the holes. In the other stages, an almost smooth decrease of the energy is observed. The end of the evolution is achieved when $F(t)$ reaches a constant value. All these features are general as they are observed also with isotropic $\gamma(\hat{\mathbf{n}})$. Furthermore, they are not affected by the specific choice of the surface energy.

From the results obtained so far we can conclude that the explicit description of the anisotropic surface energy allows for a more detailed overview of the whole evolution by surface diffusion. Moreover, it does not lead to differences in the general mechanism of coalescence, as can be easily inferred by a comparison of the simulations provided here with the evolution in the presence of isotropic surface energy in Ref. [10]. However, it is clear that the presence of facets imposes some constraints on the whole shape. For instance, in contrast to the rounding obtained with isotropic $\gamma(\hat{\mathbf{n}})$, faceted sidewalls are obtained here. As far as the coalescence occurs when sidewalls get in contact, this is expected to play a role.

In order to clarify this point we consider a simplified system made of crystals with a cylindrical shape and a height-to-base aspect ratio resembling the experimental systems of Ref. [7]. Alignment along [100] and [010] directions is considered with a gap between crystals of 0.5 μm. Then, two different $\gamma(\hat{\mathbf{n}})$ functions are selected (including some preferential orientations for Ge crystals), yielding different faceting at the sidewalls. In particular, $\gamma_1(\hat{\mathbf{n}})$ is set with $\hat{\mathbf{m}}_i$ along all ⟨111⟩ and ⟨100⟩ directions while $\gamma_2(\hat{\mathbf{n}})$ is set with $\hat{\mathbf{m}}_i$ along the directions of the same family but only with a positive

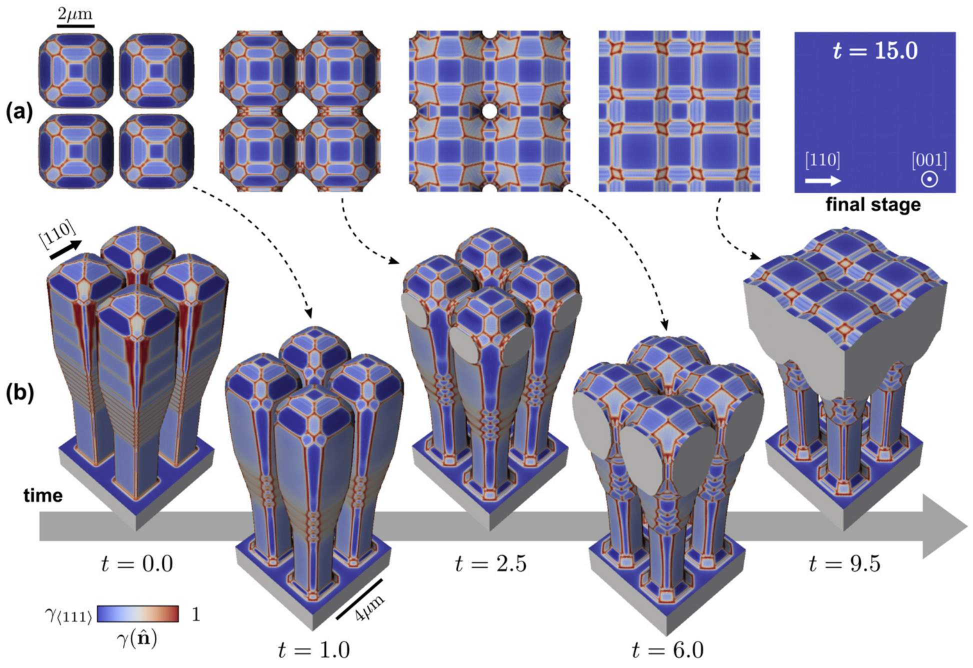

**Fig. 3.** Surface diffusion evolution by the PF simulation of closely spaced crystals. (a) Top view of the crystals at representative stages of the evolution. The last top view (upper right-hand corner) shows the final stage corresponding to the complete flattening of the suspended film. (b) Perspective view of the three-dimensional evolution. Time is expressed in arbitrary units.

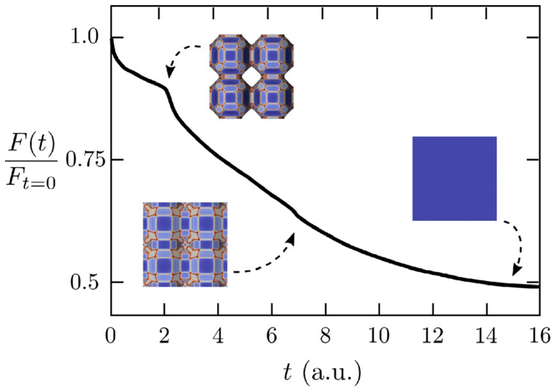

**Fig. 4.** Surface energy decrease during the evolution by surface diffusion for the simulation of crystal coalescence reported in Fig. 3. Insets show top view of the evolving morphology at representative stages.

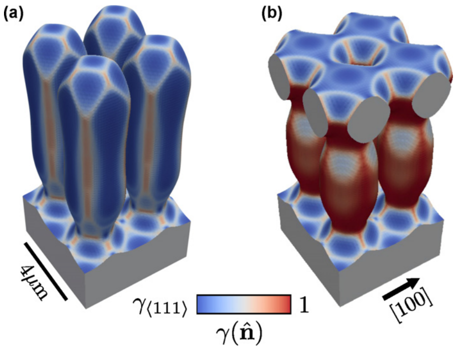

**Fig. 5.** Coalescence occurrence with different (simplified) surface energy anisotropies. The initial condition and the elapsed time is the same for both the simulations where two different $\gamma(\hat{\mathbf{n}})$ definitions are considered: (a) $\gamma_1(\hat{\mathbf{n}})$ with $\hat{\mathbf{m}}_i$ along $\langle 111 \rangle$ and $\langle 100 \rangle$ directions and (b) $\gamma_2(\hat{\mathbf{n}})$ with minima along only the $\langle 111 \rangle$ and $\langle 100 \rangle$ directions with positive component along the [001] direction. Color map shows the $\gamma(\hat{\mathbf{n}})$ values.

component along the [001] direction. For both these definitions we select $\alpha_i = 0.1$ and $w_i = 30$. This way, sidewalls are forced to exhibit $(\pm 100)$ and $(0 \pm 10)$ facets when considering $\gamma_1(\hat{\mathbf{n}})$ while they result in a rounded profile with $\gamma_2(\hat{\mathbf{n}})$. A difference in the onset of coalescence is observed when considering $\gamma_1(\hat{\mathbf{n}})$ or $\gamma_2(\hat{\mathbf{n}})$, as illustrated in Fig. 5. The elapsed time of the simulations is the same for both the panels of Fig. 5 but, while coalescence already occurred when considering $\gamma_2(\hat{\mathbf{n}})$, separated crystals are still present with $\gamma_1(\hat{\mathbf{n}})$. Therefore, when straight facets are enforced at the sidewalls, the enlargement leading to the coalescence is actually slowed down. However, in agreement with the simulations of Fig. 3, the merging of crystals is expected to occur at later stages also with $\gamma_1(\hat{\mathbf{n}})$.

## 5. Conclusions

In this work, we have theoretically investigated the morphological evolution of vertical Ge/Si heterostructures triggered by the surface diffusion mechanism in the presence of a realistic description of Ge surface-energy anisotropy [16], providing a direct application of the general formulation introduced in Ref. [22]. simulations by means of a PF model of surface diffusion were exploited to describe the 3D evolution of the Ge crystals, involving the thermodynamic faceting of the initial profile and the global morphological change of the whole microcrystals.

This investigation provided a detailed description of the expected evolution when promoting surface diffusion mechanism, e.g. when increasing the temperature during annealing experiments [10] or even when considering high temperature growth according to Ref. [25]. In particular, the evolution of isolated Ge/Si structures was shown, together with the description of the coalescence of closely spaced crystals. If the general evidence of such an evolution have been presented first in Ref. [10] by neglecting anisotropy, the present work allowed us to clarify important additional details of the evolution during annealing and to strengthen the previous theoretical analysis. In Ref. [10] lateral enlargement of the crystals during annealing was identified as the key mechanism leading to coalescence. Here, we assessed this conclusion by showing that anisotropic surface energy does not change qualitatively the process. Indeed, the presence of faceting does not fully inhibit the lateral enlargement, which determines the contact between crystals and in turn the merging of crystals. However, we also showed that tackling preferential faceting is crucial if a close comparison with experiments is desired. The presence of surface facets is found to affect the time scale of the morphological evolution and also prevents the formation of unrealistic rounded surfaces. Moreover, some features predicted by our simulations nicely reproduce fine details of the annealing experiments of Ref. [10] as, for instance, the appearance of a defined (001) facet even when considering an initial profile with a pyramid bounded by {113} facets at the top of the structures. This correspondence further confirms that the evolution of vertical Ge crystals obtained by annealing experiments is mainly determined by the activation of the surface diffusion driven by the tendency toward the minimization of the surface energy.

## References

[1] J.P. Douglas, Si/SiGe heterostructures: from material and physics to devices and circuits, Semicond. Sci. Technol. 19 (2004) R75.

[2] Y. Mo, D. Savage, B. Swartzentruber, M. Lagally, Kinetic pathway in Stranski–Krastanov growth of Ge on Si(001), Phys. Rev. Lett. 65 (1990) 1020–1023, http://dx.doi.org/10.1103/PhysRevLett.65.1020.

[3] G. Medeiros-Ribeiro, A.M. Bratkovski, T.I. Kamins, D.A.A. Ohlberg, R.S. Williams, Shape transition of germanium nanocrystals on a silicon (001) surface from pyramids to domes, Science 279 (1998) 353–355, http://dx.doi.org/10.1126/science.279.5349.353.

[4] A. Marzegalli, V.A. Zinovyev, F. Montalenti, A. Rastelli, M. Stoffel, T. Merdzhanova, O.G. Schmidt, L. Miglio, Critical shape and size for dislocation nucleation in SiGe islands on Si(001), Phys. Rev. Lett. 99 (2007) 235505–235508, http://dx.doi.org/10.1103/PhysRevLett.99.235505.

[5] E.A. Fitzgerald, Dislocations in strained-layer epitaxy: theory, experiment, and applications, Mater. Sci. Rep. 7 (1991) 87–140, http://dx.doi.org/10.1016/0920-2307(91)90006-9.

[6] D.J. Dunstan, Strain and strain relaxation in semiconductors, J. Mater. Sci. Mater. Electron. 8 (1997) 337–375, http://dx.doi.org/10.1023/A:1018547625106.

[7] C.V. Claudiu, H. von Känel, F. Isa, R. Bergamaschini, A. Marzegalli, D. Chrastina, G. Isella, E. Müller, P. Niedermann, L. Miglio, Scaling hetero-epitaxy from layers to three-dimensional crystals, Science 335 (2012) 1330–1334, http://dx.doi.org/10.1126/science.1217666.

[8] R. Bergamaschini, F. Isa, C.V. Falub, P. Niedermann, E. Müller, G. Isella, H. von Känel, L. Miglio, Self-aligned Ge and SiGe three-dimensional epitaxy on dense Si pillar arrays, Surf. Sci. Rep. 68 (2013) 390–417, http://dx.doi.org/10.1016/j.surfrep.2013.10.002.

[9] A. Marzegalli, F. Isa, H. Groiss, E. Müller, C.V. Falub, A.G. Taboada, P. Niedermann, G. Isella, F. Schäffler, F. Montalenti, H. von Känel, L. Miglio, Unexpected dominance of vertical dislocations in high-misfit Ge/Si(001) films and their elimination by deep substrate patterning, Adv. Mater. 25 (2013) 4408–4412, http://dx.doi.org/10.1002/adma.201300550.

[10] M. Salvalaglio, R. Bergamaschini, F. Isa, A. Scaccabarozzi, G. Isella, R. Backofen, A. Voigt, F. Montalenti, G. Capellini, T. Schroeder, H. von Känel, L. Miglio, Engineered coalescence by annealing 3D Ge microstructures into high-quality suspended layers on Si, ACS Appl. Mater. Interfaces 7 (2015) 19219–19225, http://dx.doi.org/10.1021/acsami.5b05054.

[11] W.W. Mullins, Theory of thermal grooving, J. Appl. Phys. 28 (1957) 333–339, http://dx.doi.org/10.1063/1.1722742.

[12] W.W. Mullins, Flattening of a nearly plane solid surface due to capillarity, J. Appl. Phys. 30 (1959) 77–83, http://dx.doi.org/10.1063/1.1734979.

[13] R. Bergamaschini, M. Salvalaglio, R. Backofen, A. Voigt, A. Montalenti, Continuum modeling of semiconducto heteroepitaxy: an applied perspective, Adv. Phys. X (2016), http://dx.doi.org/10.1080/23746149.2016.1181986, in press.

[14] M. Salvalaglio, F. Montalenti, Fine control of plastic and elastic relaxation in Ge/Si vertical heterostructures, J. Appl. Phys. 116 (2014) 104306–104314, http://dx.doi.org/10.1063/1.4895486.

[15] B. Li, J. Lowengrub, A. Voigt, Geometric evolution laws for thin crystalline films: modeling and numerics, Commun. Comput. Phys. 6 (2009) 433–482.

[16] Z. Gai, W.S. Yang, R.G. Zhao, T. Sakurai, Macroscopic and nanoscale faceting of germanium surfaces, Phys. Rev. B 59 (1999) 15230–15239, http://dx.doi.org/10.1103/PhysRevB.59.15230.

[17] A.A. Stekolnikov, F. Bechstedt, Shape of free and constrained group-IV crystallites: influence of surface energies, Phys. Rev. B 72 (2005) 125326, http://dx.doi.org/10.1103/PhysRevB.72.125326.

[18] G. Wulff, Z. Krystallogr. Mineral. 34 (1901) 449–530.

[19] C. Herring, Some theorems on the free energies of crystal surfaces, Phys. Rev. 82 (1951) 87–93, http://dx.doi.org/10.1103/PhysRev.82.87.

[20] W.C. Carter, A. Roosen, J.W. Cahn, J. Taylor, Shape evolution by surface diffusion and surface attachment limited kinetics on completely faceted surfaces, Acta Metall. Mater. 43 (1995) 4309–4323, http://dx.doi.org/10.1016/0956-7151(95)00134-H.

[21] S. Torabi, J. Lowengrub, A. Voigt, S. Wise, J. Lowengrub, A. Voigt, A new phase-field model for strongly anisotropic systems, Proc. R. Soc. A 465 (2009) 1337–1359, http://dx.doi.org/10.1098/rspa.2008.0385.

[22] M. Salvalaglio, R. Backofen, R. Bergamaschini, F. Montalenti, A. Voigt, Faceting of equilibrium and metastable nanostructures: a phase-field model of surface diffusion tackling realistic shapes, Cryst. Growth Des. 15 (2015) 2787–2794, http://dx.doi.org/10.1021/acs.cgd.5b00165.

[23] G. Russo, P. Smereka, A level-set method for the evolution of faceted crystals, SIAM J. Sci. Comput. 21 (2000) 2073–2095, http://dx.doi.org/10.1137/S1064827599351921.

[24] L.K. Aagesen, M.E. Coltrin, J. Han, K. Thornton, Phase-field simulations of GaN growth by selective area epitaxy from complex mask geometries, J. Appl. Phys. 117 (2015) 194302, http://dx.doi.org/10.1063/1.4921053.

[25] R. Bergamaschini, M. Salvalaglio, A. Scaccabarozzi, F. Isa, V.F. Claudiu, I. Giovanni, K. von, Temperature-controlled coalescence during the growth of Ge crystals on deeply patterned Si substrates, J. Cryst. Growth 440 (2016) 86–95, http://dx.doi.org/10.1016/j.jcrysgro.2016.01.035.

[26] B.J. Spencer, Asymptotic solutions for the equilibrium crystal shape with small corner energy regularization, Phys. Rev. E 69 (2004) 011603, http://dx.doi.org/10.1103/PhysRevE.69.011603.

[27] A. Rätz, A. Ribalta, A. Voigt, Surface evolution of elastically stressed films under deposition by a diffuse interface model, J. Comput. Phys. 214 (2006) 187–208, http://dx.doi.org/10.1016/j.jcp.2005.09.013.

[28] C. Gugenberger, R. Spatschek, K. Kassner, Comparison of phase-field models for surface diffusion, Phys. Rev. E 78 (2008) 016703–016719, http://dx.doi.org/10.1103/PhysRevE.78.016703.

[29] F. Chen, J. Shen, Efficient energy stable schemes with spectral discretization in space for anisotropic Cahn–Hilliard systems, Commun. Comput. Phys. 13 (2012) 1189–1208, http://dx.doi.org/10.4208/cicp.101111.110512a.

[30] S. Vey, A. Voigt, AMDiS: adaptive multidimensional simulations, Comput. Visual. Sci. 10 (2006) 57–67, http://dx.doi.org/10.1007/s00791-006-0048-3.

[31] T. Witkowski, S. Ling, S. Praetorius, A. Voigt, Software concepts and numerical algorithms for a scalable adaptive parallel finite element method, Adv. Comput. Math. 41 (2015) 1145–1177, http://dx.doi.org/10.1007/s10444-015-9405-4.

[32] R.V. Zucker, D. Chatain, U. Dahmen, S. Hagege, W.C. Carter, New software tools for the calculation and display of isolated and attached interfacial-energy minimizing particle shapes, J. Mater. Sci. 47 (2012) 8290–8302, http://dx.doi.org/10.1007/s10853-012-6739-x.

[33] L. Huang, F. Liu, G.-H. Lu, X.G. Gong, Surface mobility difference between Si and Ge and its effect on growth of SiGe alloy films and islands, Phys. Rev. Lett. 96 (2006) 016103, http://dx.doi.org/10.1103/PhysRevLett.96.016103.